Journal of Applied Mechanics and Technical Physics, Vol. 50, No. 2, pp. 309–317, 2009

GAS-DYNAMIC SIGNS OF EXPLOSIVE ERUPTIONS OF VOLCANOES.
2. MODEL OF HOMOGENEOUS–HETEROGENEOUS NUCLEATION.
SPECIFIC FEATURES OF DESTRUCTION OF THE CAVITATING MAGMA

V. K. Kedrinskii

UDC 532.593+532.529+532.528+532.787+550.3

The dynamics of state of the crystallite-containing magma is studied within the framework of the gas-dynamic model of bubble cavitation. The effect of crystallites on flow evolution is considered for two cases: where the crystallites are cavitation nuclei (homogeneous–heterogeneous nucleation model) and where large clusters of crystallites are formed in the magma in the period between eruptions. In the first case, decompression jumps are demonstrated to arise as early as in the wave precursor; the intensity of these jumps turns out to be sufficient to form a series of discrete zones of nucleation ahead of the front of the main decompression wave. Results of experimental modeling of an explosive eruption with ejection of crystallite clusters (magmatic "bombs") suggest that a cocurrent flow of the cavitating magma with dynamically varying properties (mean density and viscosity) transforms to an independent unsteady flow whose velocity is greater than the magma flow velocity. Experimental results on modeling the flow structure during the eruption show that coalescence of bubbles in the flow leads to the formation of spatial "slugs" consisting of the gas and particles. This process is analyzed within a combined nucleation model including the two-phase Iordansky–Kogarko–van Wijngaarden model and the model of the "frozen" field of mass velocities in the cavitation zone.

Key words: *magma, dynamics of state, gas-dynamic model, nucleation, decompression wave.*

The present paper describes the dynamics of the magma flow structure studied in model experiments and the gas dynamics of its bubble state in decompression waves.

1. Specific Features of the Structure of the Bubble Cavitation Zone under the Conditions of Homogeneous–Heterogeneous Nucleation. As was noted in [1, 2], cavitation nuclei can form on crystallites whose volume concentration can be substantially greater than the concentration of gas nuclei; as a result, heterogeneous nucleation proceeds in the melt, in addition to homogeneous nucleation. The gas-dynamic model proposed in [3], which describes the above-mentioned processes, remains valid. The specific feature of the physical formulation of the problem is the fact that the heterogeneous mechanism is "triggered" in each layer after the homogeneous nucleation is completed; at this moment, the initial sizes of all nuclei, regardless of their nature, are assumed to be identical.

It follows from calculations (see the initial conditions in [3]) that the flow structure becomes significantly different if the model of homogeneous–heterogeneous nucleation is used. As in usual bubble and cavitating media [4], the incident wave (either a shock wave or a rarefaction wave) is divided into a precursor with the front 1 [curve $P(x)$ in Fig. 1a] propagating in a homogeneous medium with a velocity of sound c_0 and the main perturbation with the front 2 propagating in a bubble medium with a phase velocity of sound $c_{\rm ph}$. The emergence of heterogeneous nuclei in the melt leads to an increase in their total density by one or two orders, as compared with the case of homogeneous nucleation. The precursor structure becomes substantially different, and its profile in the vicinity

---

Lavrent'ev Institute of Hydrodynamics, Siberian Division, Russian Academy of Sciences, Novosibirsk 630090; kedr@hydro.nsc.ru. Translated from Prikladnaya Mekhanika i Tekhnicheskaya Fizika, Vol. 50, No. 2, pp. 167–177, March–April, 2009. Original article submitted June 4, 2008.

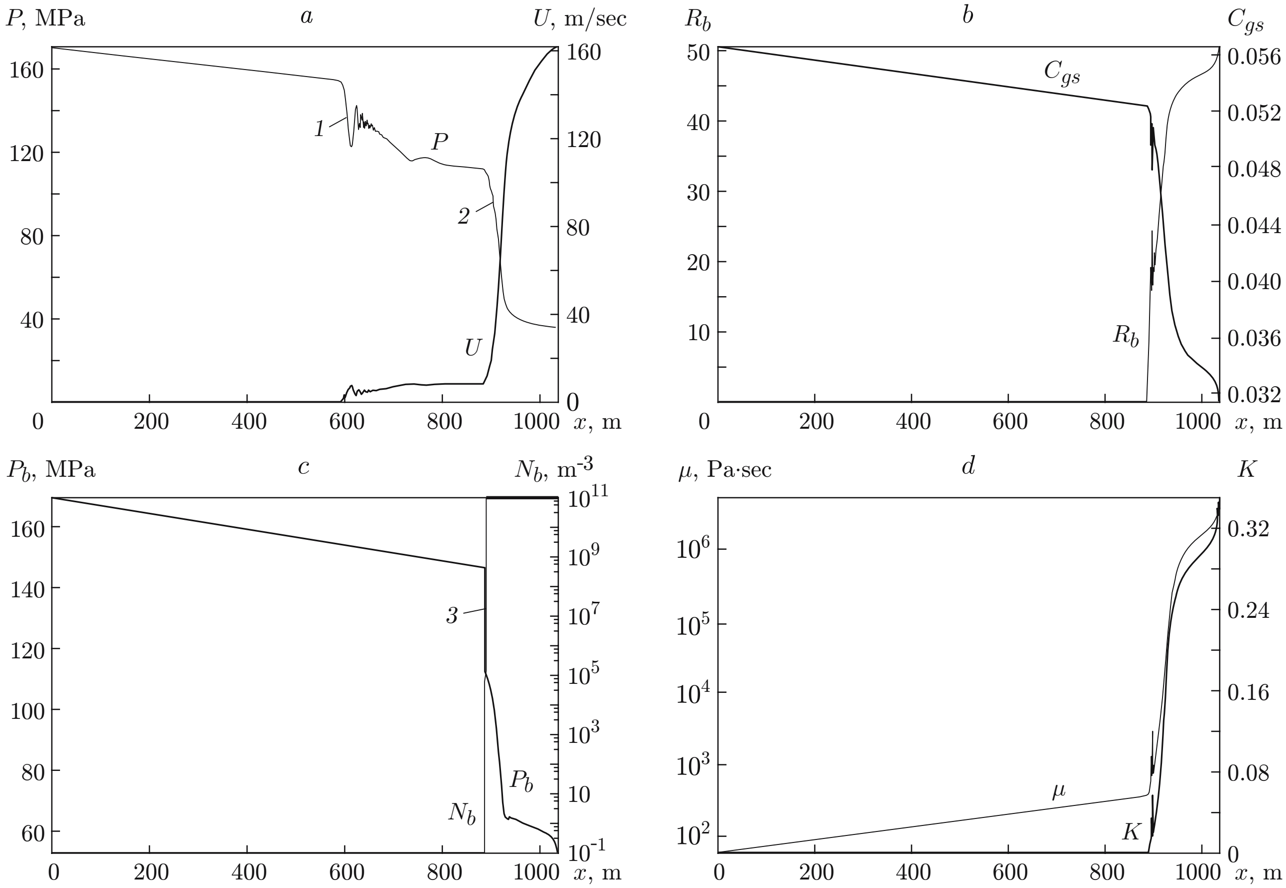

Fig. 1. Distributions of the main characteristics of the dynamics of state of the melt along the magma column at $t = 0.25$ sec: (a) pressure in the decompression wave P and mass velocity U; (b) concentration of the dissolved gas C_{gs} and bubble radius R_b; (c) pressure in the cavitation bubbles P_b and concentration of nuclei N_b; (d) viscosity of the melt μ and volume concentration of the bubbles K; 1) precursor front; 2) front of the main perturbation; 3) decrease in pressure in the bubbles on the front of the zone of saturation by the nuclei in the main decompression wave.

of the front 1 becomes oscillating [curve $P(x)$ in Fig. 1a]. The front 2 of the main decompression wave moves considerably slower; by $t = 0.25$ sec, it covers a distance of 100 m only from the initial upper level of the magma column [curve $P(x)$ in Fig. 1a]. Note that the distribution of the mass velocity $U(x)$ has the same two characteristic segments as the decompression wave.

Thus, at $t = 0.25$ sec, the precursor structure has a high-frequency component in the vicinity of the front and a low-frequency component with a significantly varying amplitude on the segment between the magma-column levels of 600 and 900 m. For this reason, obviously, the pressure in this zone of the melt decreases and reaches a level sufficient for the phase transition and saturation of the melt by bubble nuclei. The calculations reveal a jump in concentration on the saturation front to the maximum level $N_b = 10^{11}$ m^{-3} and a drastic decrease in pressure in the nuclei on the front approximately by 40 MPa [segment 3 on the curve $P_b(x)$ in Fig. 1c]. Jumps also appear in the distributions of the main characteristics of the melt (Figs. 1b and 1d).

It follows from the calculation results that the presence of an oscillating structure of the precursor is responsible for a drastic change in the melt state at $t = 1.5$ sec: spontaneous emergence of discrete zones 4 of saturation of the melt by the nuclei ahead of the front 2 of the main wave and the corresponding changes in the distributions of the parameters P_b, μ, R_b, C_{gs}, and K (Fig. 2) are observed. The number of discrete zones for all the indicated characteristics of the melt state ahead of the decompression-wave front reaches the maximum value at this time instant. Discrete zones of reduced (as compared with the pressure corresponding to the static distribution) pressure P_b in the cavitation bubbles appear in all zones of saturation by the nuclei ahead of the decompression-wave front.

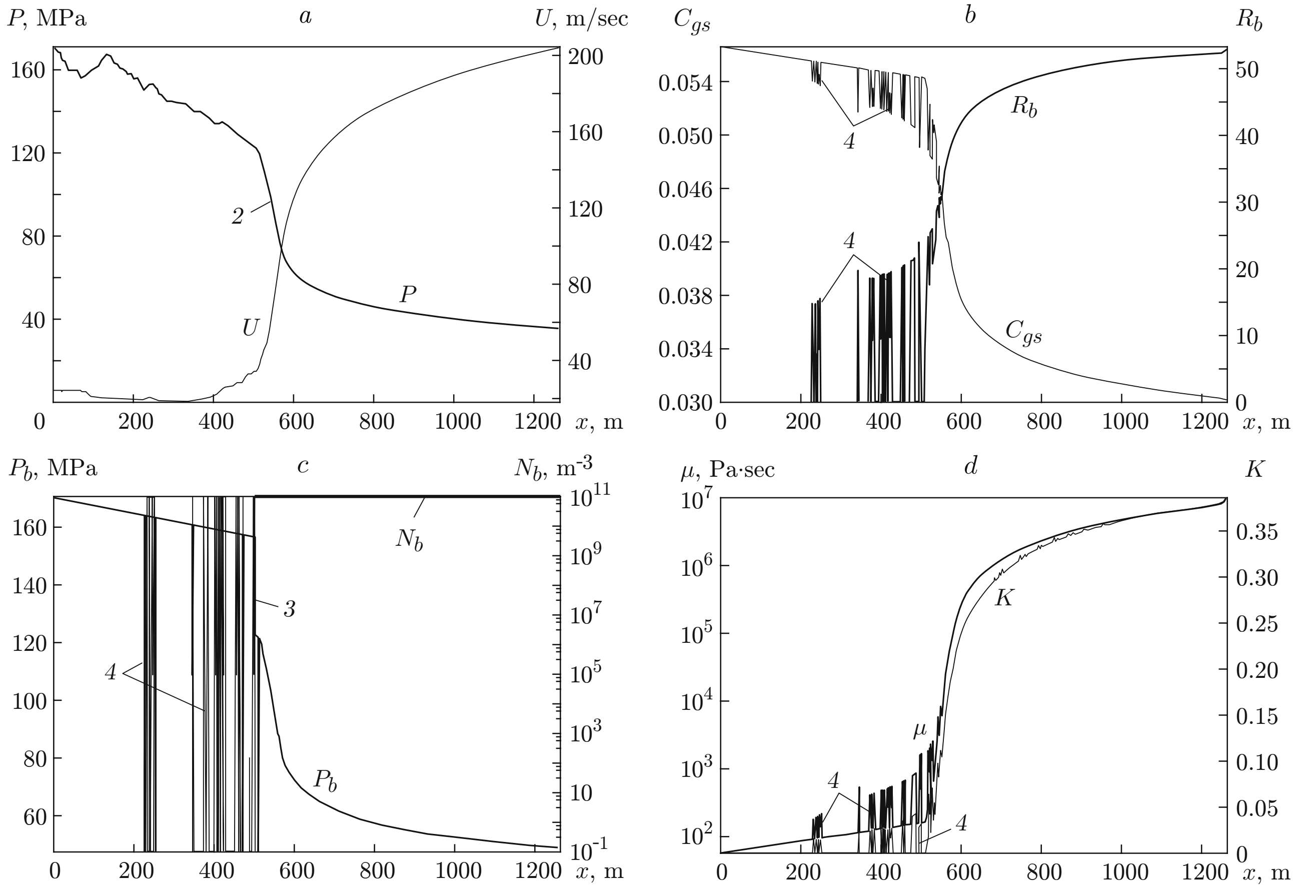

Fig. 2. Distributions of the melt characteristics P and U (a), C_{gs} and R_b (b), P_b and N_b (c), μ and K (d) along the magma column at $t = 1.5$ sec: 2) front of the main perturbation; 3) decrease in pressure in the bubbles on the front of the zone of saturation by the nuclei in the main decompression wave; 4) system of discrete zones behind the precursor front.

In Fig. 2c, these zones merge with the curves N_b, and the presence of these zones is manifested only as an increased thickness of the curves N_b.

It should be noted that the pressure in the cavitation bubbles near the free boundary of the magma column remains rather high (up to 50 MPa), and the bubble radii (50 μm) are greater than the radii predicted by the homogeneous model, because of the initial stage of cavitation development in the precursor (Fig. 2c). The concentration of the gas dissolved in the melt decreases to 3%, while the concentration of the vapor bubbles reached 35%. Later on, as the decompression wave propagates inward the magma column, the discrete cavitation zones ahead of the wave front merge together and disappear. By the time $t = 2.6$ sec, the distributions of all the main characteristics become continuous again. The decompression-wave front is registered near the coordinate $x = 200$ m, the height of the magma column increases up to 1.5 km owing to cavitation processes, and the distribution of viscosity of the liquid component of the melt has an insignificant gradient in the interval $x = 400$–1500 m: the viscosity μ changes in the interval $3 \cdot 10^5$–10^7 Pa·sec.

2. Crystal Clusters in the Cavitating Magma (Experimental Modeling). A combined structure of the eruption is known to be typical for some types of volcanoes; in this case, the eruption is accompanied by powerful ejection of hot magma “bombs” to a height of several kilometers and by a lava flow [5]. Such a flow structure allows us to assume that the magma in the volcano channel in the period between the eruptions is a strongly crystallized melt, with possible spontaneous formation of crystal clusters and glass-transition zones.

This state can be considered as a metastable state with a nonuniform (in terms of density) distribution of the crystal phase (clusters). In the case of sudden decompression initiating an explosive eruption, the process of intense nucleation can be expected to proceed both in the magma and in the liquid component of the crystal cluster.

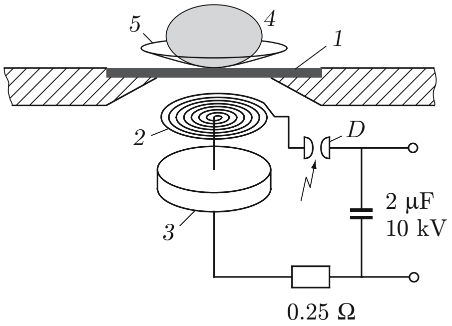

Fig. 3

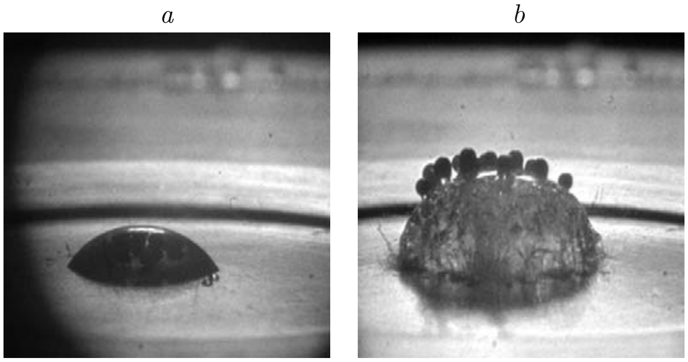

Fig. 4

Fig. 3. Sketch of the electromagnetic hydrodynamic shock tube: 1) conducting membrane; 2) flat spiral; 3) copper disk; 4) liquid drop; 5) annular cumulative jet; the discharge gap is indicated by D.

Fig. 4. Initial stage of separation into two flows under shock-wave loading of a three-phase system (liquid drop with suspended particles): $t = 0$ (a) and 180 μsec (b).

Thus, in the case of a combined eruption, the magma flow can be considered as a three-phase medium consisting of the magma proper, bubble zones, and crystals, as well as vitreous crystallized clusters (with probable existence of internal cavitation zones).

The dynamics of state of this medium under pulsed decompression was modeled in experiments with a system consisting of a liquid, cavitation nuclei, and non-wettable solid particles. For this purpose, we used mixtures of arbitrarily shaped solid particles 1–3 mm with a solution of colophony in acetone or with distilled water containing natural microinhomogeneities in the form of gaseous nuclei with a density up to 10^{12} m^{-3}. In the latter case, the suspended state of the particles was provided by adding glycerin.

Laboratory modeling was performed by the method of consecutive (shock wave — rarefaction wave) loading of a drop of the mixtures mentioned above (with a diameter of approximately 1 cm) on an electromagnetic hydrodynamic shock tube (Fig. 3). This method offers a unique possibility of real-time realization of pulsed processes in the examined sample, which are adequate to natural effects in many aspects. As the real liquid (such as distilled water) contains microinhomoheneities with a density of approximately 10^{12} m^{-3} [6], small volumes of the liquid can be used as samples to be tested. For example, a liquid drop with a 0.5-cm radius contains potential nucleation centers with a density approximately equal to 10^{11} m^{-3}. This means that samples of these volumes can be considered as typical elements of the examined medium. Thus, the scale of the process (but not the process itself) can be substantially changed, and a necessary resolution of the fine structure of the flow can be reached. Note that the use of a laser pulse with a duration of about 3 nsec for illumination allowed us to resolve the fine structure of the flow: a thin annular cumulative jet in the form of a sheet arising due to the diaphragm impact on the drop (Fig. 3).

The main objective of the study was to analyze the dynamics of formation of the three-phase flow structure to gain better understanding of interaction between the solid particles in the flow and the bubble clusters formed behind the front of the rarefaction waves. The experiments showed that destruction of the three-phase magma can be primarily caused by separation of the magmatic "bombs" into an independent flow moving with a high velocity and by destruction of the cavitating magmatic melt at the stage of the development of its foam structure (Figs. 4–6). The photographs in Fig. 4 show the initial shape of the drop with solid particles inside the drop and the initial stage of separation of the flows of the particles and the cavitating liquid. As is seen from the experiments, the solid particles moving with a significantly greater velocity are ejected from the general flow and form a system, which is practically independent of the cavitating liquid (zoom-in image in Fig. 5). In the experiments, the volume concentration of the solid particles in the mixture N_p changed from $N_p = 5$–6% to $N_p = 80\%$ (see Figs. 4–6).

The experimental research of the influence of the solid phase concentration on the dynamics of the three-phase flow revealed that, as the concentration of the particles increases, they become entrained into the formation of the cellular flow structure, being mainly distributed along the boundaries of liquid cells (Figs. 6b and 6c). When the concentration reaches $N_p \approx 60\%$, the particles themselves actually form the cellular structure of the drop. This

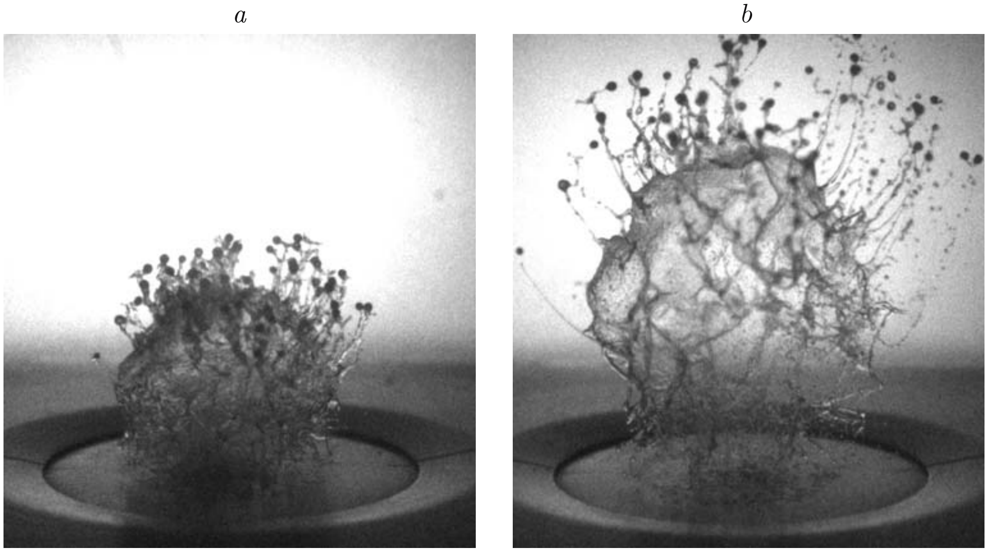

Fig. 5. Formation of the flow of solid particles and their ejection from the cavitating drop: $t = 10^3$ μsec (a) and $1.5 \cdot 10^3$ μsec (b).

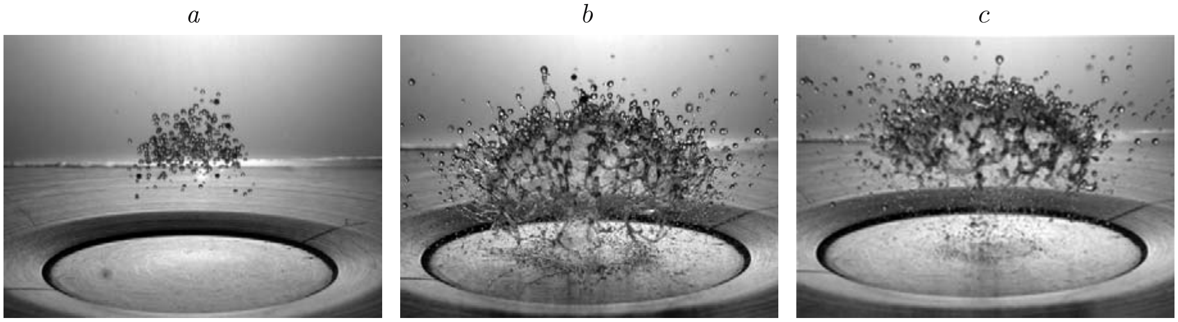

Fig. 6. Effect of the particle concentration on the structure of the three-phase drop under shock-wave loading: “dry” cloud of particles (a) and $N_p = 20$ (b) and 40% (c).

conclusion is supported by the flow structure with a low volume concentration (see Fig. 5): the particle flow is ejected from the main flow together with cell elements, which “accompany” the particle flow in the form of liquid tails. The photograph in Fig. 6a (taken with an exposure time of about 1 μsec) shows one of the states of the “drop” of dry particles. It is seen that its structure remains compact under shock-wave loading with the same parameters.

We can easily see that the process of separation of the three-phase flow formed under shock-wave loading of a liquid drop is determined by the specific features of motion of the solid phase in the cavitating medium. The experiments performed with a group of 3 to 5 particles mixed in different proportions (in terms of volume) with a liquid demonstrated, in particular, that the dynamics of ejection of single particles is consistent with the results described above. It should be noted that the mathematical model taking this process into account is considerably more complicated than the known classical problems of hydrodynamics of the flow around a sphere. The sphere moves in a medium with an intensely developing cavitation process and phase transitions.

An analysis of experimental data on the mechanism of separation of the three-phase flow into two almost independent flows allows us to conclude that it is necessary to formulate a more general problem of unsteady motion of a solid sphere in a cocurrent flow with dynamically changing properties (mean density and viscosity). It should be noted that the system of kinetic relations (1)–(7) in [3] and the two-phase Iordansky–Kogarko–van Wijngaarden (IKW) model in this formulation should be considered as the basic equations, which allow one to determine the dynamics of state of the medium where the particle motion is considered. Actually, the solution of this problem is expected to determine the kinetics of phase separation in a three-phase flow with crystal clusters.

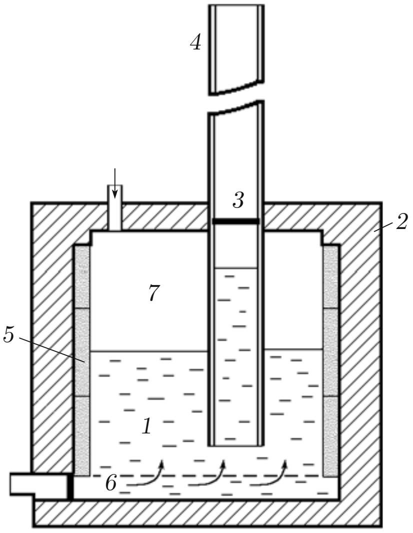

Fig. 7. Modified Glass–Heuckroth scheme: 1) examined liquid; 2) high-pressure chamber; 3) gate; 4) plane rectangular channel; 5) thermal heaters; 6) system for saturation of the liquid by carbon dioxide; 7) gas compressed to high pressure.

According to the results in Figs. 3 and 4 in [3], an approximately 40% volume concentration of the vapor–gas phase is established in the cavitation zone in the height range $x = 600$–1300 m and remains practically invariable in the time interval $t = 1.5$–6.0 sec. This value of the concentration corresponds to a rather dense packing of bubbles, and the magma acquires a foam state. One of the currently accepted models of the eruption [7–9] predicts that the foam structure of the magma appears directly before magma fragmentation.

It is assumed that foam destruction is governed by inversion of the two-phase state: transition from the cavitating liquid to the state of the gas–particle type. Such a model *a priori* implies a uniform distribution of all parameters of the medium in closely located cross sections of the channel (size of cavitation bubbles, their volume concentration, viscosity, and mass velocity), but ignores the coalescence (random process of bubble merging, obviously violating the uniform distributions of parameters), which is possible due to such density of bubbles. A question arises: Can the general mechanism determining the structure at the final stage of the eruption (structure of ejection) be expected to be valid in this case? Let us consider the specific features of the dynamics of cavitating magma destruction.

3. Hydrodynamic Shock Tubes as a Method of Modeling the Dynamics of the Flow Structure in Decompression Waves. The eruption process was modeled in a modified analog of the Glass–Heuckroth tube (see [3]), which includes a high-pressure chamber and a plane channel with a rectangular cross section separated by a gate, thermal heaters, and a system for saturation of the sample of the examined liquid by carbon dioxide (Fig. 7). The space above the liquid sample surface is filled by the gas up to a prescribed pressure; the channel is connected to the evacuation system.

Figure 8 shows the typical eruption structures registered (with a microsecond exposure) in the atmosphere near the channel exit (Figs. 8a and 8b) and inside the channel (Fig. 8c) for liquids with viscosities differing by orders of magnitude. Figure 8a shows the structure of the liquid flow with a viscosity $\mu \approx 0.2$ Pa $\cdot$ sec ($T = 19$°C) at the time t_1 and its variation in the interval t_1–t_2. At the initial stage of destruction, the transition of the cavitating liquid to a foam structure, which is typical for water [10], is also observed for a liquid whose viscosity is higher by two orders of magnitude (frame I in Fig. 8a). The microsecond exposure allowed us to resolve the fine flow structure, which changes substantially with time: the flow becomes stratified into a system of three-dimensional vertical jets (frame II in Fig. 8a). As the viscosity of the destroyed liquid is further increased by one more order of magnitude ($\mu \approx 2.6$ Pa $\cdot$ sec and $T = 42$°C), the flow becomes almost completely stratified and acquires a more definite jet-like character (see Fig. 8b).

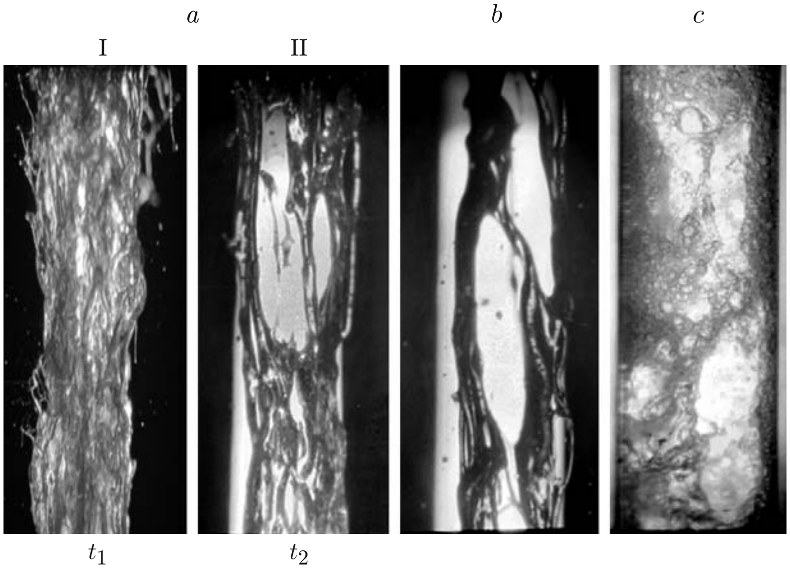

Fig. 8. Flow structure directly above the channel exit (a and b) and in the channel with a system of "slugs" (c): (a) liquid with a viscosity $\mu = 0.2$ Pa · sec at the times t_1 (I) and $t_2 > t_1$ (II); (b) liquid with a viscosity $\mu = 2.6$ Pa · sec.

A probable reason for this effect was determined by studying the dynamics of the flow structure in the low-velocity regime of the eruption of saturated liquids directly in the tube channel (see Fig. 7). For usual water ($\mu = 0.001$ Pa · sec), the structure of the low-velocity eruption includes a system of up-floating dense bubble clusters whose state is close to foam (see Fig. 8c). The foam structure is spontaneously destroyed in some clusters owing to bubble coalescence, and zones ("slugs") filled by the vapor–gas mixture with liquid particles are formed; the flow structure gradually turns into a combined "slug"–bubble cluster system (see Fig. 8c). For the solution with a viscosity higher by three orders of magnitude, the flow-structure dynamics is basically the same as that for water (only the time scale changes). Registration (with a microsecond exposure) of the flow structure in the channel directly before the eruption in the explosive regime (see Fig. 8c) confirms its combined character in the inviscid liquid as well.

Under these conditions, it is not a system of individual bubbles that explode near the magma surface. The exploding objects are macrovolumes of three-dimensional "slugs" containing a gas–particle mixture formed as a result of an "internal cavitation explosion." Obviously, the three-dimensional "slugs" are formed in various regions of the magma flow and float up to the magma surface with different velocities and from different depths. The formation of such a chain of macrovolumes in the magma flow and their consecutive explosive destruction can be considered as one possible mechanism of periodic ejection of the gas–particle mixture during the explosive eruption of a volcano. A question arises: Is it possible to construct a mathematical model that provides a qualitative description of the "internal cavitation explosion" by using the ideas about the most typical processes associated with the dynamics of state of the cavitating liquid and the structure of the wave field in this liquid?

4. Physicomathematical Model of the "Internal Cavitation Explosion." Experimental investigations of liquid destruction in intense rarefaction waves yielded an unexpected (at first glance) result: a quasi-steady field of mass velocities is formed in cavitation zones as the volume concentration of the gas phase increases [11]. It turned out that this effect appears owing to relaxation of tensile stresses, which can be described by the two-phase IKW model of the wave-field structure dynamics in a developed cavitation zone [12]. These two effects (stress relaxation and "frozen" field of mass velocities) form the basis of the so-called combined mathematical model, which allows the evolution of cavitation processes to be studied up to the moment when the two-phase medium passes to a foam-like state.

The essence of the combined model implies that the dynamics of state of the field of tensile stresses, their relaxation, the field of mass velocities, and the developing cavitating process are numerically analyzed within the

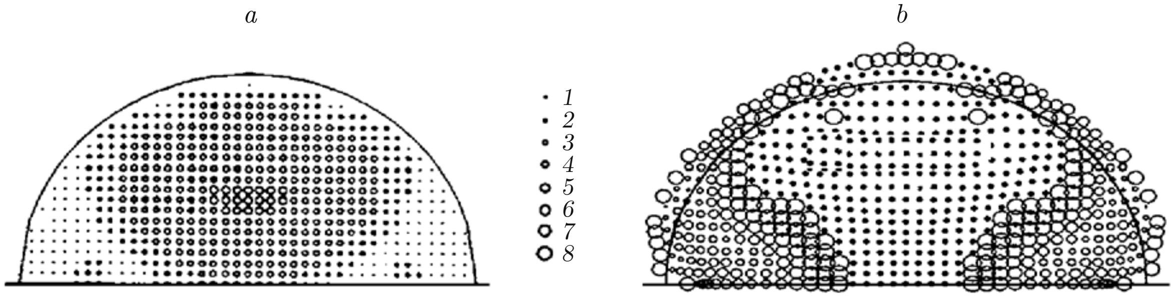

Fig. 9. Formation of a gas–drop “slug” as a result of the “internal cavitation explosion” for $t = 40.5$ (a) and 145 μsec (b): $R = 0.01$ (1), 0.03 (2), 0.05 (3), 0.08 (4), 0.1 (5), 0.13 (6), 0.15 (7), and 0.2 cm (8).

framework of the nonequilibrium two-phase IKW model:

$$u_t = \rho^{-1} p_\zeta, \qquad \rho^{-1} = \rho_0^{-1} x_\zeta, \qquad x_t = u,$$
$$R R_{tt} + (3/2) R_t^2 = \rho_l^{-1} (p_g - p), \tag{1}$$
$$p_g = p_0 (R/R_0)^{3\gamma}, \qquad k = k_0 (R/R_0)^3, \qquad \rho = \rho_l (1 - k).$$

Here, the conservation laws are written in the Lagrangian mass coordinates; the subscript t indicates the corresponding partial derivatives with respect to time; x and ζ are the Eulerian and Lagrangian coordinates, respectively. The calculations with the use of system (1) are performed until a state is reached where the tensile stresses in the medium can be neglected, and the field of mass velocities reaches a quasi-steady regime. At the next stage, the field of mass velocities is “frozen,” and the main characteristic of the cavitation zone becomes its mean density. The system of equations governing further evolution of cavitation becomes substantially simplified and acquires the form

$$(\rho^{-1})_t = \rho_0^{-1} u_\zeta, \qquad u_t = 0, \qquad x_t = u, \qquad p = p_0, \qquad \rho^{-1} = \rho_{l,0}^{-1} + v_b,$$

where v_b is the volume of the cavitation bubbles in a unit mass of the mixture.

A numerical analysis of the dynamics of the liquid drop structure under shock-wave loading within the framework of the combined model was performed in [13] for the case of drop loading by a shock wave with an amplitude $p_{\max} \approx 15$ MPa and a positive phase $\tau_+ \approx 3$–5 μsec. It turned out that a dense cavitation zone is developed at the drop center in the region of tensile stresses. At the time $t = 40.5$ μsec after the beginning of loading, the size of the cavitation bubbles in this zone reaches the visible size or becomes even greater (Fig. 9a). At $t = 145$ μsec, a gas–particle “slug” is formed at the drop center owing to coalescence of the bubbles and subsequent formation and destruction of the foam structure (Fig. 9b). It follows from the results of the numerical analysis that the boundary of this “slug” moves with a velocity of the order of the mass velocity behind the front of the incident shock wave, thus, “capturing” the surrounding zones of the cavitating medium. This evolving process can be defined as the “internal cavitation explosion.”

Conclusions. The effect of crystallites on the dynamics of state of the magma is studied within the framework of a gas-dynamic model of bubble cavitation. Decompression jumps, dense spectra of discrete cavitation zones, nucleation zones, and jumps in viscosity and concentration are demonstrated to appear already in the wave precursor ahead of the main wave front in the case of homogeneous–heterogeneous nucleation with crystallites acting as cavitation nuclei.

It follows from the results of experimental modeling of the explosive eruption with ejection of crystallite clusters (magmatic “bombs”) that the latter move in a cocurrent flow of the cavitating magma with dynamically changing properties (mean density and viscosity) with a velocity greater than the magma velocity and form a flow independent of the magma flow. It is shown that coalescence of the bubbles leads to the formation of three-dimensional “slugs” consisting of the gas and particles. This process is analyzed within the framework of a combined model including the IKW model and the model of the “frozen” field of mass velocities in the cavitation zone.

This work was supported by the Russian Foundation for Basic Research (Grant No. 06-01-00317) and by the Integration Project No. 4.14.4 of the Siberian Division of the Russian Academy of Sciences.

REFERENCES

1. M. Manga, H. M. Gonnermann, and A. Namiki, "Why do volcanoes (only sometimes) erupt explosively?" in: *Abstracts of the Canad. Geophys. Union and Amer. Geophys. Union Meeting*, Montreal (2004).
2. A. Namiki and M. Manga, "Importance of preexisting bubbles for volcano explosivity," in: *Abstracts of the Canad. Geophys. Union and Amer. Geophys. Union Meeting*, Montreal (2004).
3. V. K. Kedrinskii, "Gas-dynamic signs of explosive eruptions of volcanoes. 1. Hydrodynamic analogs of the pre-eruption state of volcanoes, dynamics of the three-phase magma state in decompression waves," *J. Appl. Mech. Tech. Phys.*, **49**, No. 6, 891–898 (2008).
4. V. K. Kedrinskii and S. I. Plaksin, "Rarefaction wave structure in cavitating liquid," in: *Proc. of the 11th Int. Symp. on Nonlinear Acoustics* (Novosibirsk, August 24–28, 1987), Vol. 1, Sib. Branch USSR Acad. Sci., Novosibirsk (1987), pp. 51–55.
5. D. P. Hill, F. Pollitz, and Ch. Newhall, "Earthquake–volcano interactions," *J. Phys. Today*, **55**, No. 11, 41–47 (2002).
6. A. S. Besov, V. K. Kedrinskii, and E. I. Pal'chikov, "Studying of the initial stage of cavitation using the diffraction-optical method," *Pis'ma Zh. Tekh. Fiz.*, **10**, No. 4, 240–244 (1984).
7. A. W. Woods, "The dynamics of explosive volcanic eruptions," *Rev. Geophys.*, **33**, No. 4, 495–530 (1995).
8. F. Dobran, "Non-equilibrium flow in volcanic conduits and application of the eruption of Mt. St. Helens on May 18 1980 and Vesuvius in Ad. 79," *J. Volcanol. Geotherm. Res.*, **49**, 285–311 (1992).
9. A. R. Berngardt, E. I. Bichenkov, V. K. Kedrinskii, and E. I. Pal'chikov, "Optic and x-ray investigation of water fracture in rarefaction wave at later stage," in: *Proc. of the IUTAM Symp. on Optical Methods in the Dynamics of Fluids and Solids* (Prague, September 17–21, 1984), Springer, Berlin (1985), pp. 137–142.
10. V. K. Kedrinskii, "Nonlinear problems of cavitation breakdown of liquids under explosive loading (review)," *J. Appl. Mech. Tech. Phys.*, **34**, No. 3, 361–377 (1993).
11. A. R. Berngardt, "Dynamics of the cavitation zone in the case of cavitation destruction of water," in: *Dynamics of Continuous Media* (collected scientific papers) [in Russian], No. 104, Inst. Hydrodynamics, Sib. Div., Russian Acad. of Sci., Novosibirsk (1992), pp. 3–15.
12. V. K. Kedrinskii, "Negative pressure profile in cavitation zone at underwater explosion near free surface," *Acta Astronaut.*, **3**, Nos. 7/8, 623–632 (1976).
13. M. N. Davydov, "Mathematical modeling of evolution of cavitation clusters in a liquid under pulse loading," Candidate's Dissertation in Physics and Mathematics, Novosibirsk (2006).